Role of substrate and annealing temperature on the structure of ZnO and $Al_xZn_{1-x}O$ thin films for solar cell applications

Fred Joe Nambala[1,2] , Jacqueline M. Nel[1], Augusto G. J. Machatine[1], Bonex W. Mwakikunga[3], Eric G. Njoroge[1] Kelebogile Maabong[1,4], Arran G.M. Das[5], Mmantsae Diale[1, *]

[1]*Department of Physics, University of Pretoria, Private bag X20, Hatfield, 0028. South Africa.*
[2]*Department of Physics, University of Zambia, PO Box 32379, Great East Road Campus, Lusaka. Zambia.*
[3]*DST/CSIR National Centre for Nano-Structured Materials, PO Box 395, Pretoria South Africa.*
[4]*Physics Department, University of Botswana, Private Bag 0022, Gaborone, Botswana.*
[5]*Monash University, Private Bag X60, Roodepoort 1725, South Africa.*
**Corresponding author e-mail address: mmantsae.diale@up.ac.za*

ABSTRACT

This paper reports on the deposition of pure and 5 at.% Al doped ZnO (AZO) prepared by sol-gel and applied to the substrates by spin-coating, and the role of annealing temperature on the crystallinity of these layers. It is found that both ZnO and AZO are largely amorphous when coated on glass compared to n-Si(111), as substrates. On both substrates, X-ray diffraction (XRD) shows that the crystallinity improves as annealing temperature is raised from 200 to 600 °C with better crystallinity on Si substrates. The thickness of the films on substrates was determined as 120 nm by Rutherford backscattering spectroscopy (RBS). Specular ultra-violet visible (UV-vis) gives the direct transition optical band gaps (E_g) for AZO as-deposited films are 2.60 and 3.35 eV while that of 600 °C annealed films are 3.00 and 3.60 eV. The E_g calculated from diffuse reflectance spectroscopy (DRS) UV-vis are more diverse in ZnO- and AZO-Si than the ZnO- and AZO-glass samples, although in both sets the E_g tend to converge after annealing 600 °C. The Raman spectra of samples show multiphonon processes of higher order from the AZO and substrates. It is found that residual stresses are related to E_2 Raman mode.

Keywords: AZO, annealing, Raman spectroscopy, spin-coating, substrate, sol-gel

1. Introduction

Transparent conductive oxides (TCO) films are extensively used in optoelectronic devices such as organic light emitting diodes (OLED), liquid crystals display (LCD) and solar cells [1-4]. Thus far, indium tin oxide (ITO) film has been the preferred choice for TCO materials [5], because of its high stability and low resistivity. However, ITO has become a rare commodity because the supply of indium is rapidly diminishing from nature, thus making it very expensive.

ZnO has recently been developed as an ideal alternative material for ITO due to its low cost, easy synthesis and growth, and wide availability. Research reveals that Al, B, Ga, Mn, Co and F doped ZnO films show low resistivity and high transmittance [5-9]. In addition, to obtain high quality ZnO films, a variety of growth techniques may be used such as molecular beam epitaxy (MBE), pulse laser deposition (PLD), RF magnetron sputtering, reactive DC sputtering and sol-gel. Based on the previous literature, Al seems to be a successful and promising doping element for ZnO [8, 10-12]. Al can be substitutionally incorporated at the Zn lattice site in the ZnO structure, denoted as AZO [13], to fabricate Al doped ZnO film with high temperature stability and good immunity against hydrogen plasma reduction [14-

16].

Hong *et al.* reported that AZO does not degrade the active solar cell material by the inter-diffusion of constituents as it occurs for ITO films [7]. However, optoelectronic devices require thermal treatments during fabrication. Therefore, the TCOs must maintain their properties throughout such high temperature processes. Thus, the study of the effects of thermal treatment on the structural and optical properties of TCOs demands high consideration for optoelectronic applications of these films. In this work, we report on the preparation of sol-gel ZnO and AZO thin films as-deposited and annealed at 600 °C with the Al concentration of 0 and 5 at.%, respectively, as well as the role played by glass and Si substrates. The structural and optical properties of the films were investigated using X-ray diffraction (XRD), specular and diffuse reflectance spectroscopy (DRS) ultra-violet visible (UV-vis), Rutherford backscattering spectrometry (RBS), and Raman spectroscopy**.**

2. Materials and Experimental Techniques

Undoped ZnO nanoparticles were synthesized using appropriate quantities of aqueous zinc acetate dehydrate, 2-methoxyethanol and ethanolamine by sol-gel method. A calculated quantity of aluminium nitrate nonahydrate was added to the sol-gel preparation to obtain 5 at.% of Al in ZnO. The reaction solutions were maintained at 70 °C for 2 hr while being stirred continuously. Glass and crystalline Si substrates were all degreased by consecutive sonication for 5 min in trichloroethylene, 2-propanol and methanol [1]. The glass substrates were finally rinsed with de-ionised (DI) water before blow-drying them with nitrogen (N_2) gas. The n-Si(111) substrates were rinsed with de-ionised (DI) water, etched with 40% hydrofluoric acid (HF) and then rinsed again in DI water after which they were blow-dried with N_2 gas. Thin films of 5 layers were then deposited by spin-coating at 3000 rpm for a minute on both glass and n-Si(111) the day after sol-gel preparation and films were pre-heated at 200 °C for 2 min between layers. Post-annealing was done at 200 and 600 °C for 1 hr, respectively, in a flowing nitrogen:oxygen mix ((N_2:O_2) 2:1 ratio).

XRD measurements were carried out using a PANalytical X'Pert Pro powder diffractometer in theta/theta configuration with an X'Celerator detector and variable divergence, and fixed receiving slits with Fe filtered Co $K_{\alpha 1}$ radiation (wavelength, λ=1.789 Å). The phases were identified using X'Pert Highscore plus software. Additional XRD measurements were conducted using Rigaku smartLab XRD instrument operated in out-of-plane mode, with Cu $K_{\alpha 1}$ radiation wavelength of 1.54 Å, in theta/2-theta configuration with a Sc-70 detector. The voltage was 45 kV, current 200 mA and the scan speed was 2 deg/min. RBS measurements were carried out using a collimated He^+ beam. The incident energy of He^+ beam on the samples was 1.6 MeV. The backscattered particles were collected using a surface barrier detector placed at 165° with a target current of ~15 nA and charge of ~ 8 μC. Spectral UV-vis measurements were performed using the Cary 100 Bio UV-visible spectrophotometer. DRS UV-vis measurements were conducted using a Cary 400 UV-visible spectrophotometer. Micro-Raman spectroscopy was performed using a T64000 Raman spectrograph (Horiba Jobin Yvon, France). A 514.6 nm laser line from a mixed gas Krypton-Argon laser (Coherent) was used as excitation source. The power of the laser at the sample

was 10 mW using 32.0 A operating the laser at 150 mW in order to minimize localized heating of the sample. An LD 50× objective fixed to an Olympus microscope was used to obtain spectra under two acquisitions of 250 s with a spectral resolution of ~ 2 cm^{-1}.

3. Results and discussion

3.1 X-Ray Diffraction (XRD)

Figures 1 and 2 show ZnO on n-Si(111) and glass substrates, respectively. The spectra in Figure 1 indicates that the Si(111) peak at 33.00° has a high intensity and further goniometer out-of-plane XRD measurements on the sample could damage both the Rigaku instrument and X'Celerator detector. Hence, only the ZnO as-deposited on n-Si(111) sample was analysed and shows a prominent peak at 41.00° indexed as (002) reflection. In Figure 2, the ZnO as-deposited on glass shows a broad peak from 17.00° to 30.00° which is characteristic of the glass substrate. Figure 2(b) presents peaks at 38.00°, 41.50° and 43.00° for the ZnO annealed at 600 °C indexed as (100), (002) and (110) reflections, respectively, using the ICSD card number 164690. The ZnO as-deposited on glass and Si substrates spectra both show an unknown peaks at 52.50°.

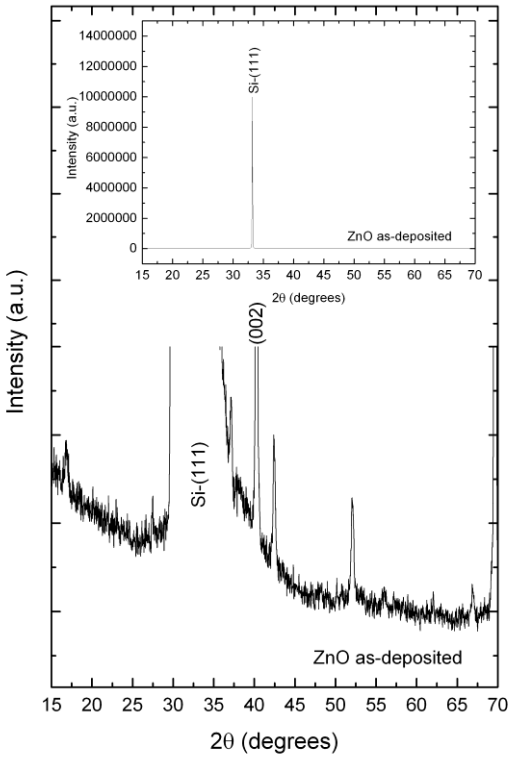

Figure 1: Rigaku smartLab XRD instrument pattern for ZnO on n-Si(111) using copper (Cu) $K_{\alpha 1}$ radiation source for as-deposited films. Spectra were changed to cobalt (Co) $K_{\alpha 1}$ radiation using the Highscore plus software. The insert shows high intensity counts for the as-deposited films on Si sample due to single crystalline material which could damage an XRD instrument's detector. The unlabelled peaks are unknown.

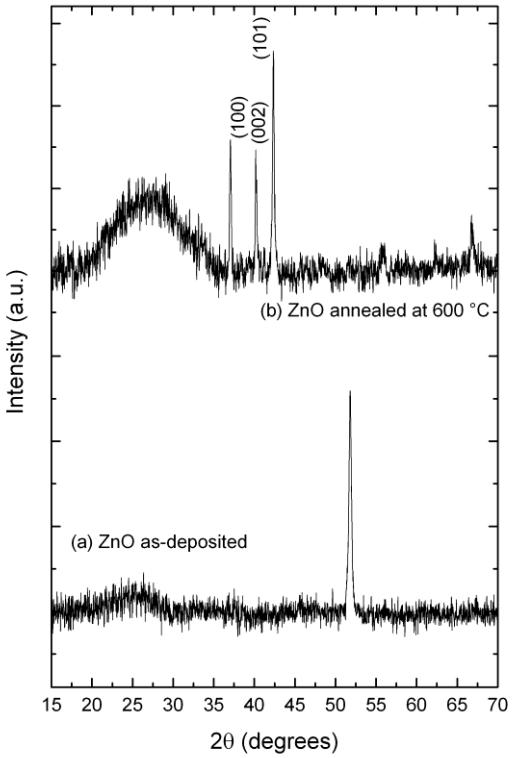

Figure 2: XRD patterns of ZnO on glass using copper (Cu) $K_{\alpha 1}$ radiation source for (a) as-deposited films and (b) 1 hr annealed at 600 °C films. Rigaku smartLab XRD instrument's spectra were changed to cobalt (Co) $K_{\alpha 1}$ radiation using the Highscore plus software. The peak at 52° on the as-deposited spectra is unknown.

For the AZO on n-Si(111) substrate, diffraction peaks at 30.00° and 33.00° were observed as illustrated in Figure 3. Using the inorganic crystal structure database (ICSD) card number 34927, the peak at 33.00° is assigned to the (111) reflections of Si while the peak at 30.00°is an artifact. As-deposit ١ and annealed at 200 °C for 1 hr AZO films on Si show a very low intensity peak at 39.00° reflection emanating from the Si substrate and not the AZO material. Figure 3 also shows XRD patterns at various stages of the AZO films' processing on Si(111) sustrates. AZO films annealed at 600 °C show (002) reflection at 40.30° corresponding to the ICSD card number 164690. The crystallite size D was found to be 17.10 nm using the Debye-Scherrer equation [1]

$$D = \frac{0.9\lambda}{\beta \cos\theta} \tag{1}$$

where β is the full-width at half-maximum (FWHM) of the peak, λ is the wavelength and theta θ is the Bragg angle. As the annealing temperature of the material increases, the crystallinity of the film increases and the (002) peak dominates and the Si peaks become weaker.

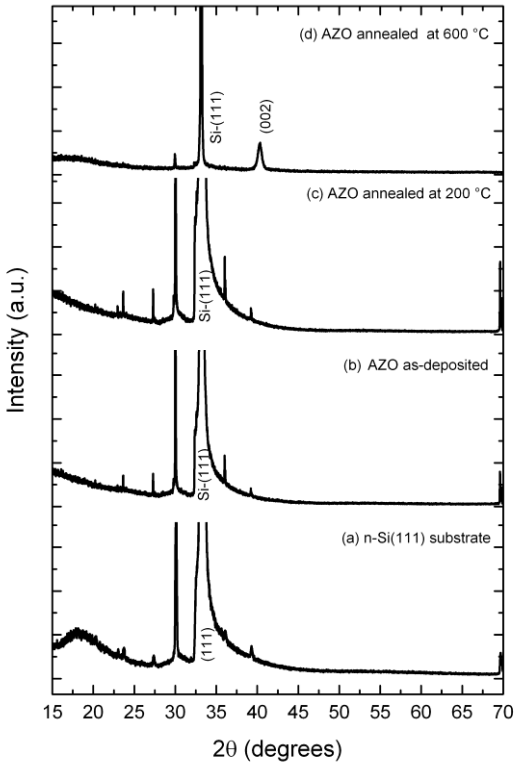

Figure 3: PANalytical X'Pert Pro XRD pattern for 5 at.% Al-ZnO on n-Si(111) using cobalt (Co) $K_{\alpha 1}$ radiation source for (a) substrate Si, (b) as-deposited films, (c) 1 hr annealed at 200 °C films and (d) 1 hr annealed at 600 °C.

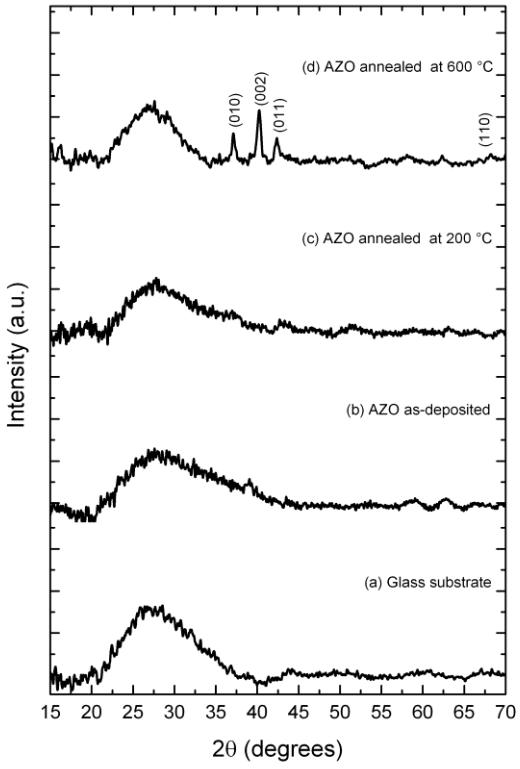

Figure 4: PANalytical X'Pert Pro XRD pattern for 5 at.% Al-ZnO on glass using cobalt (Co) $K_{\alpha 1}$ radiation source for (a) substrate glass, (b) as-deposited films, (c) 1 hr annealed at 200 °C films and (d) 1 hr annealed at 600 °C.

For glass substrates, Figure 4 shows 3 peaks (010), (002) and (011) at 38.00°, 40.20° and 42.00° after annealing at 600 °C. The prominent peak of the AZO films was indexed as (002) reflection at 40.20° which gives 19.00 nm as crystallite.

The determined crystallite sizes are similar to those obtained by Muiva *et al.* who used same method of sample preparation [17].

For the (002) reflection, using

$$a = \sqrt{\frac{1}{3}}\frac{\lambda}{\sin\theta},\ c = \frac{\lambda}{\sin\theta} \tag{2}$$

for the hexagonal structure [18], the a and c lattice parameter values for AZO were calculated as 0.300 and 0.519 nm for n-Si(111) substrate, and 0.301 and 0.521 nm for glass

substrate compared to the single crystal ZnO with 0.325 and 0.520 nm. The c/a were determined as 1.7321 for AZO on n-Si(111), and 1.7321 for AZO on glass. These values correspond to the doped ZnO nanostructures of wurtzite/hexagonal crystal structure with $P6_3mc$ (C^4_{6V}) space group [19]. It can be seen that values obtained for a are slightly smaller than those for pure ZnO, but the c values are very close to those of pure ZnO. This results in c/a being larger than that for pure ZnO indicating that Al is in a substitutional position.

The interplanar spacing, *d*, for wurtzite structure is obtained by the Bragg's law given by

$$\frac{1}{d^2} = \frac{4}{3}\left(\frac{h^2 + hk + k^2}{a^2}\right) + \frac{l^2}{c^2} \tag{3}$$

where *h*, *k* and *l* are Miller indices denoting the structure's plane [17, 20]. The d values for AZO films were determined as 0.260 nm for n-Si(111) and 0.261 nm for glass substrates. Using the (002) reflection, the d value for single crystal ZnO is 0.260 nm [20].

3.2 Rutherford backscattering spectroscopy (RBS)

RBS was used to calculate the thicknesses of the ZnO and AZO thin films deposited on Si substrates using RUMP code [21] on raw RBS spectra data. The RBS spectra of the as-deposited ZnO on n-Si(111) (i.e., ZnO-Si as-deposited in Figure 5(a)) and annealed at 600 °C aluminium doped ZnO on n-Si(111) (i.e., Al-ZnO-Si 600 °C annealed in Figure 5(b)) with associated simulations are presented in Figure 5. The arrows in the RBS spectra figures represent surface positions of Zn, O and Si. The spectra data simulations of as-deposited ZnO and AZO films on n-Si(111) provided thicknesses of 120 nm with a composition of 46 and 54 at.% of Zn and O, respectively.

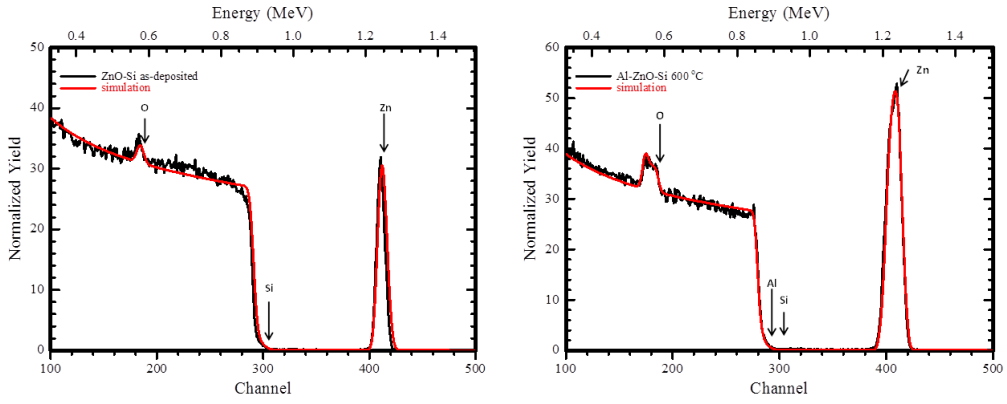

(a) ZnO on n-Si(111) as-deposited. (b) AZO on n-Si(111) annealed at 600°C. The

Figure 5: RBS raw and simulation data for undoped ZnO and 5 at.% Al in AZO on n-Si(111) annealed at 600 °C. The AZO as-deposited RBS was essentially same as the ZnO as-deposited result.

After annealing the Al-ZnO-Si sample at 600 °C, an interfacial layer of about 40 nm was detected between the Si substrate and AZO films. This layer consisted of a mixture of Zn, O and Si with compositions of 10, 80 and 10 at.% respectively. The initial layer of 80 nm consisted of Zn and O in 46 and 54 at.% respectively which indicated an almost 1:1 stoichiometry. The composition of the top layer had not changed compared to the as-deposited sample. The 5 at.% Al in the AZO films on Si substrate sample was not detected by RBS. This could be due to the obscuring of Al by the Si peak. The obtained 120 nm thickness for the films on Si substrate was used for both DRS and specular UV-vis data analyses – upon extending it to ZnO as well as AZO films on glass samples.

3.3 Ultra-violet Visible (UV-vis)

3.3.1 Specular/Transmission

In order to elucidate optical band gaps we employ the well-known Tauc equation [17] given as

$$(\alpha h\nu)^n = E_g - h\nu \tag{4}$$

where α is the absorption coefficient, h is the Planck's constant, E_g is the optical band gap of the material in the thin film, v is the frequency and $n = 2$ for direct band gap material. The α is related to transmittance (T) as follows: $\alpha = {}^{1}\!/_{t} \ln(1/T(\%))$ where t is the thickness of the thin film. The thickness of the ZnO and AZO thin films on n-Si(111) substrates determined by RBS was used to calculate the absorption coefficient for glass substrates' films. The E_g for undoped ZnO as-deposited on glass films was determined as 3.25 eV whereas the E_g values of the 5 at.% Al-ZnO as-deposited on glass films were determined as 2.60 and 3.35 eV as shown in Figure 6(a). The 2.60 eV Eg is attributed to the defects that exist in the band gap of ZnO. For the ZnO on glass 600 °C annealed films, the E_g value was determined as 3.25 eV as shown in Figure 6(b). The AZO on glass 600 °C annealed films E_g values are 3.00 and 3.60 eV (seen Figure 6(b)). The 3.60 eV E_g is very high compared to the standard ZnO E_g 3.37 eV ZnO [22, 23]. The E_g values of AZO films on glass substrates are comparable to those determined with DRS UV-vis measurements shown in figures 7(a) and 7(b). Govender *et al.* showed that a high transparency material, i.e., tungsten trioxide, in the spectral region with two varying thicknesses of a 750 nm difference gives E_g values that are only 0.05 eV different [24]. Therefore, the closeness in E_g values of AZO on glass obtained by specular and DRS UV-vis leads to a conclusion that the RBS measured AZO on n-Si(111) thickness can be extended to the experimental AZO films on glass substrates since the sample preparation procedure was same. Table 1 illustrates the E_g values of ZnO and AZO of this study.

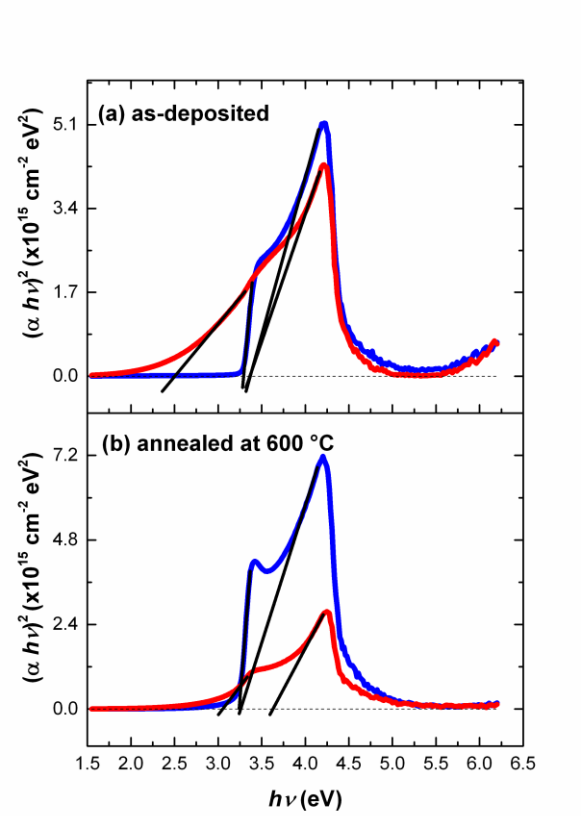

Figure 6: Specular UV-vis results showing optical band gaps where black linear lines cut the *hv*-axis. The blue curves indicate ZnO measured results while the red curves present those for 5 at.% Al in AZO on glass films. (a) As-deposited and (b) annealed at 600 °C films.

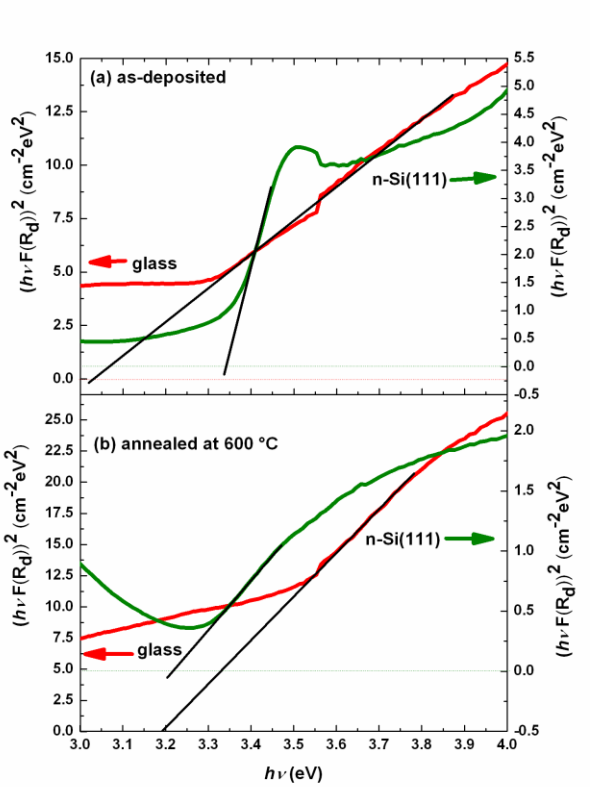

Figure 7: Diffuse Reflectance Spectroscopy (DRS) UV-vis for 5 at.% Al in AZO on glass and Si substrates. Optical band gaps are shown where black linear lines cut the *hv*-axis. Green and red curves indicate measured results for films on Si and glass substrates. (a) As-deposited and (b) annealed at 600 °C films.

3.3.2 Diffuse Reflectance Spectroscopy (DRS)

AZO films on glass and n-Si(111) substrates, respectively, were characterised using DRS UV-vis by applying the Kulbeka-Munk function. The reflectance data obtained can be used to acquire information on the proportion of incident photons that are absorbed, and hence the optical band gap energy of the material in the sample. The Kubelka-Munk equation [21, 25, 26] relates the reflectance to absorption coefficient and is given as

$$\frac{\alpha}{S} = \frac{(1-R)^2}{2R} \tag{5}$$

where α is the absorption coefficient, S is the scattering coefficient and R is the reflectance. Diffuse reflectance signal, R_d, which is essentially R of a layer that is thick enough to completely mask the substrate relates to absorbance A as $A = -\log(R_d)$ [21, 26]. Combining equations 4 and 5, one can get

$$\left(S\frac{(1-R)^2}{2R}h\nu \right)^n = E_g - h\nu \quad (6)$$

The scattering coefficient, *S*, can be wavelength dependent. However it is known that for particle size greater than 5 μm, *S* can be wavelength independent [13]. We also assumed that *S* is wavelength independent since the beam size impinges on larger than 1 mm in the far field. Consequently, the detector in the DRS UV-vis observes a wavelength independent scattering from the nano-structured surface.

The E_g values for 5% Al-ZnO on glass films were determined for the as-deposited and annealed at 600 °C films. In Figure 7(a) the as-deposited AZO on glass E_g is 3.03 eV. For the same AZO composition deposited on n-Si(111), an E_g value of 3.34 eV for the as-deposited film was obtained. For the films annealed at 600 °C on glass and Si substrates, the E_g values were determined as 3.19 and 3.22 eV, respectively, presented in Figure 7(b). Clearly, the mean value of E_g AZO is slightly less than 3.37 eV obtained for pure ZnO [22, 23]. Table 1 shows the determined E_g values.

3.4 Raman spectroscopy

The space group of Al doped ZnO is similar to that of bulk crystalline ZnO. The space group of bulk wurtzite ZnO (w-ZnO) is C^4_{6V} ($P6_3mc$). There are 12 phonons, three acoustic (LA + 2TA) and nine optical (LO, TO) modes [2, 27].

The six Raman active first order modes for the undoped ZnO, in cm^{-1}, are: $A_1(TO)$ = 381, $A_1(LO)$ = 574, $E_1(TO)$ = 407, $E_1(LO)$ = 583, $E_2(low)$ = 101 and $E_2(high)$ = 437. The silent modes have Raman shift B'_1 = 260 cm^{-1} and B'_2 = 540 cm^{-1}. Selection rules and momentum conservation of the phonon modes determine the symmetry of phonons in a crystal [28].

Figure 8 shows the as-deposited undoped ZnO and AZO films on both glass and Si substrates. The ZnO and AZO on n-Si(111) as-deposited spectra are similar due to the substrate. However, the ZnO and AZO on glass as-deposited spectra are different in that 989 cm^{-1} peak in Figure 8(b) is not as prominent in Figure 8(d). Also, in the AZO on glass as deposited spectra, the 383 cm^{-1} peak is present with the undoped 437 cm^{-1} peak shifting to 440 cm^{-1}.

In Figure 9, the films annealed at 600 °C are shown. Doping introduces defects, strains and stresses that may lower the symmetry of a crystal or allow modes that are forbidden by symmetry to be observed. Figures 9(b) and 9(d) show the AZO films data deconvolution (by applying Lorentzian multiple peak fit) using Origin Lab Software giving Raman bands [29]. Figure 9(b) shows the Raman peaks at 407, 440, 576 and 976 cm^{-1} for undoped ZnO on glass. The spectra show multiphonon peaks and is modulated by broader phonon peaks of armophous glass structure, centred around 788 and 1096 cm^{-1}. The 575 cm^{-1} peak is assigned to $A_1(LO)$ phonon of ZnO zone center (Γ-point) [9]. Thus, the additional overtone and combination modes which originate from ZnO are $2E_2$ = 2×101 cm^{-1} = 202 cm^{-1}, $A_1(LO)+E_1(LO)$ = 1149 cm^{-1}, 434 cm^{-1} (101+334) cm^{-1}, 668 cm^{-1} (2×334 cm^{-1}). The 334 cm^{-1} mode has been observed by many authors [9, 30, 31] but its origin is still under discussion although it clearly follows the $A_1(TO)$ mode [32].

As in the as-deposited ZnO and AZO films on Si substrate case, the annealed at 600 °C ZnO and AZO films on Si do not show deviations from each other (see figures 9(a) and 9(c)). However, the annealed at 600 °C ZnO and AZO films on glass substrates results are different. Also, when the ZnO films on glass are annealed, a new peak at 407 cm^{-1} appears in comparison to spectra in Figure 8(b). Figure 9(d) shows that the annealing at 600 °C of AZO on glass films causes material to have a peak at 418 cm^{-1} in contrast to the two peaks in the as-deposited AZO films on glass in Figure 8(d).

In figures 8(a), 8(c), 9(a) and 9(c), the broad peak starting at 1050 cm^{-1} with a peak at 1085 cm^{-1} (~2×542 cm^{-1} at M-point) can be assigned as B_2 (high) forbidden which is intrinsic to impurity in the growth of crystal ZnO [33, 34]. The peak observed at 651 – 656 cm^{-1} is related to Al doping [2, 4]. The much higher frequency 1455 cm^{-1} originates from the combination ~A_1(LO)+E_1(TO)+E_2(high).

In AZO as-deposited (Figure 8(d)) and annealed at 600 °C (Figure 9(d)) films on glass substrates, we observe additional peaks from the fundamental mode frequencies, i.e., the first-order Raman modes [9, 33].

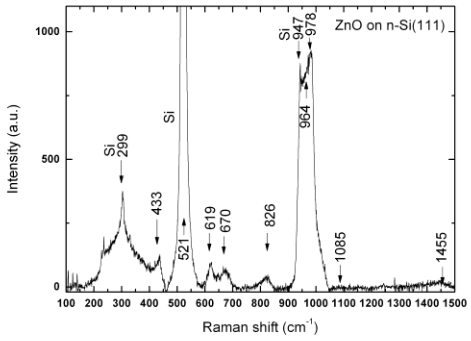

(a) ZnO on n-Si(111)

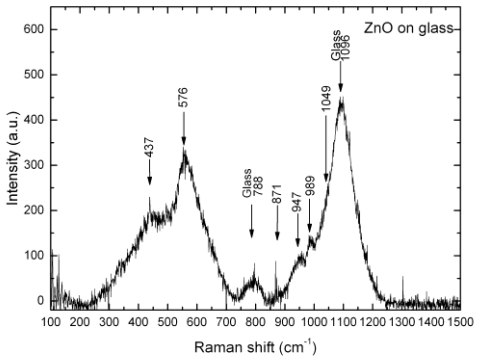

(b) ZnO on glass

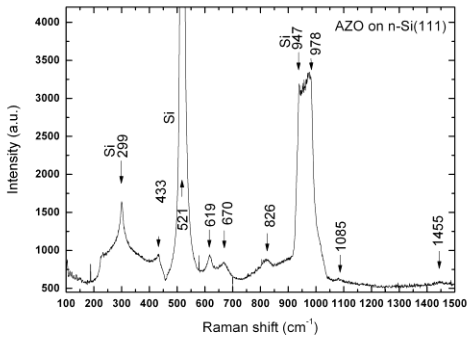

(c) AZO on n-Si(111)

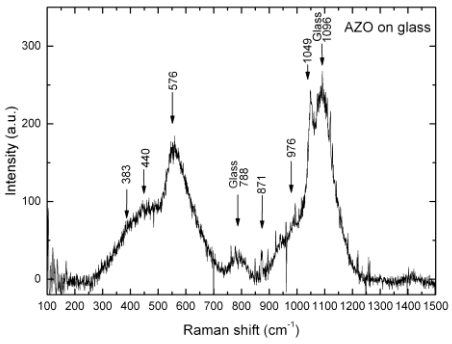

(d) AZO on glass

Figure 8: ZnO and AZO films as deposited on glass and Si substrates. The Raman spectra for ZnO and AZO films on glass substrates are similar to that in Figure 9 which shows the deconvoluted peaks.

Similarly, for AZO on n-Si(111) substrates after annealing at 600°C, as shown in Figure 8(c), we observed multiphonon peaks originating from the substrate, 299, 521 and 947 cm^{-1} = LO(L) + LA(L) + TA(X). The mode at Γ-point may originate from the edge of the Brillouin zone (BZ) of Si $W^1 \otimes W^1$ = LO + LA or $W^2 \otimes W^2$ = TO + LO; TA + LA can be assigned frequencies 940 – 956 cm^{-1}. The L, X, W are high symmetry points in the Si O_h^7 – space group [28] since the laser light reaches the Si substrate.

The AZO broader peaks emanate from low crystallinity and mismatch of ZnO on Si(111) at 16,6% [35].

Yahia *et al.* reported that the E_2 vibration mode at 440 cm^{-1} is characteristic of the wurtzite phase of ZnO and that stress induced in the wurtzite crystals affects the E_2 phonon frequency [36]. The E_2(high) mode is blue shifted in AZO to 440 cm^{-1} (Figure 8(b)) and used as a measure of residual stress [2, 36]. In the AZO on Si substrate, we observe E_2(high) 433 cm^{-1} which indicates residual stress in ZnO films probably due to the n-Si(111) substrate [36].

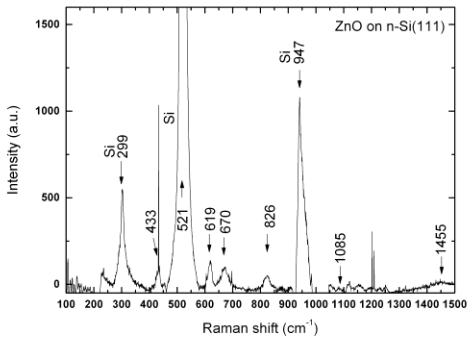

(a) ZnO on n-Si(111)

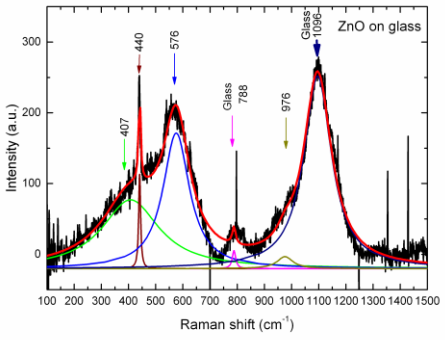

(b) ZnO on glass

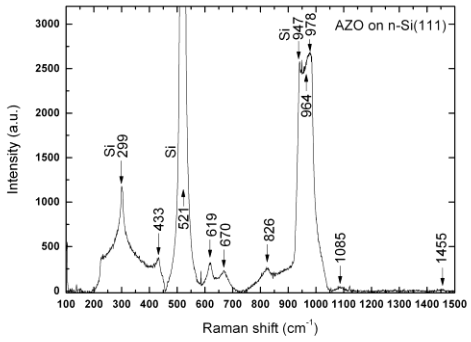

(c) AZO on n-Si(111)

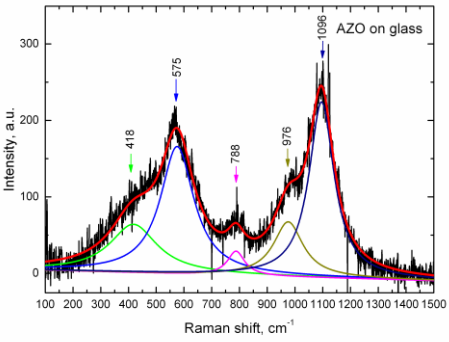

(d) AZO on glass

Figure 9: ZnO and AZO films annealed at 600°C on glass and Si substrates, respectively. The Raman spectra for ZnO and AZO on glass are similar to those in Figure 8.

4. Conclusion

The properties of sol-gel prepared ZnO and 5 at.% Al doped ZnO thin films on glass and Si substrates, respectively, were investigated using XRD, RBS, DRS and specular UV-vis, and Raman. Films deposited on glass provided the characteristic properties of the prepared ZnO and AZO materials. The ZnO and AZO films deposited on n-Si(111) substrates present effects that result due to the interface between the prepared materials and Si. For all XRD measurements, the (002) is the most preferred orientation of the films on both substrates although peaks for (010), (011) and (110) orientations were also observed in the XRD pattern for glass substrates samples. XRD of AZO thin films shows a decrease in the value of lattice parameter a compared to that of pure ZnO indicating that Al is in a substitutional position as opposed to interstitial. The thickness of ZnO and AZO films on glass and Si substrates were determined to be 120 nm using RBS. The determined average E_g results for ZnO and AZO on glass substrates indicate that values generally become higher after thermal treatment at 600 °C. From both DRS and specular UV-vis, the direct transition E_g values were found to be approximately 3.37 eV for a pure ZnO crystal. These values are consistent with the trend of reducing E_g value as the concentration of Al increases from 0 to 5 at.% in the $Al_xZn_{1-x}O$ polycrystalline material configuration. The Raman spectra have shown shifts in the E_2 frequency which indicates residual stresses in the ZnO films probably due to mismatch between Si substrate and ZnO/AZO films [9]. Yahia *et al.* indicated that glass has peaks at 790 and 1072 cm^{-1} as well as ZnO bulk at 578 and 1150 cm^{-1} [36]. Raman modes close to these have been observed. The peaks are broad indicating low crystallinity. Raman spectra reveal multiphonon processes of the thin films on glass and Si substrates. A symmetry assignment of first order Raman modes of Al-ZnO on glass and n-Si(111) was discussed.

Acknowledgements

The authors acknowledge Jack Madito for valuable discussion, Wiebke Grote of University of Pretoria and Mohammed Khenfouch of University of South Africa for the XRD instrument issues as well as spectra discussions, and Dr S Radhakrishnan for the specular UV-vis work. The work was financially supported by the University of Pretoria, the South African National Research Foundation (NRF), Project #79177; National Science and Technology Council (NSTC), Project #10168; and Energy and Environmental Research group (EERG) of the University of Zambia.

References

[1] R. Vinodkumar, K.J. Lethy, P.R. Arunkumar, R.R. Krishnan, N.V. Pillai, V.P.M. Pillai, R. Philip, Materials Chemistry and Physics, 121 (2010) 406-413.
[2] S.-S. Lo, D. Huang, C.H. Tu, C.-H. Hou, C.-C. Chen, Journal of Applied Physics, 42 (2009).
[3] S. Mondal, K.P. Kanta, P. Mitra, Journal of Physical Sciences, 12 (2008) 221-229.
[4] F.J. Manjon, B. Mari, J. Serrano, A.H. Romero, Journal of Applied Physics, 97 (2005) 053516.
[5] M.-C. Jun, J.-H. Koh, Journal of Electrical Engineering Technology, 8 (2013) 163-167.
[6] K.T. Igamberdiev, S.U. Yuldsashev, T.W. Kang, V.O. Pelenovich, Journal of the Korean Physical Society, 55 (2009) 934-937.

[7] R.J. Hong, X. Jiang, G. Heide, B. Szyszka, V. Sittinger, W. Werner, Journal of Crystal Growth, 249 (2003) 461-469.
[8] F. Maldonado, A. Stashans, Journal of Physics and Chemistry of Solids, 71 (2010) 784-787.
[9] S.S. Shinde, C.H. Bhosale, K.Y. Rajpure, Spectrochimica Acta Part A: Molecular and Biomolecular Spectroscopy, 98 (2012) 453-456.
[10] T.H. Khume, M.N.M. Yusuf, B. Ismail, Y. Wahab, Z. Othaman, Proceedings of Annul Fundamental Science Seminar AFSS 2006, 2006 pp. 6-7.
[11] W.W. Liu, B. Yao, Z.Z. Zhang, Y.F. Li, B.H. Li, C.X. Shan, J.Y. Zhang, D.Z. Shen, X.W. Fan, Journal of Applied Physics 109 (2011) 093518 -093518-093515.
[12] D. Raoufi, T. Raoufi, Applied Surface Science 255 (2009) 5812-5817.
[13] S.-Y. Tong, J.-M. Wu, Y.-T. Huang, M.-D. Yang, M.-J. Tung, Journal of Applied Physics D: Applied Physics, 43 (2010) 445502.
[14] K. Ellmer, Journal of Physics D: Applied Physics, 33 (2000) R17.
[15] J.F. Chang, M.H. Hon, Thin Solid Films, 386 (2001) 79-86.
[16] T. Minami, T. Miyata, T. Yamamoto, Journal of Vacuum Science & Technology A, 17 (1999) 1822-1826.
[17] C.M. Muiva, T.S. Sathiaraj, K. Maabong, Ceramics International 37 (2011) 555-560.
[18] Y. Ammaih, A. Lfakir, B. Hartiti, A. Rudah, P. Thevenin, M. Siadat, Opt Quant Electron, 46 (2014) 229-234.
[19] Z.K. Heiba, L. Arda, Crystal Research and Technology, 44 (2009) 845-850.
[20] G.S. Thool, A.K. Singh, R.S. Singh, A. Gupta, M.A. Bin Hasan Susan, Journal of Saudi Chemical Society, 18 (2014) 712-721.
[21] L.R. Doolittle, Nuclear Instruments and Methods in Physics Research Section B: Beam Interactions with Materials and Atoms, 9 (1985) 344-351.
[22] A. Mondal, N. Mukherjee, S.K. Bhar, Materials Letters, 60 (2006) 1748 - 1752.
[23] W. Mtangi, F.D. Auret, C. Nyamhere, P.J. Janse van Rensburg, A. Chawanda, M. Diale, J.M. Nel, W.E. Meyer, Physica B, (2009).
[24] M. Govender, B.W. Mwakikunga, A.G.J. Machatine, H.W. Kunert, Physica status solidi C, 211 (2014) 349.
[25] T.J. McCarthy, S.P. Ngeyi, J.H. Liao, D.C. DeGroot, T. Hogan, C.R. Kannewurf, M.G. Kanatzidis, Chemistry of materials, 5 (1993) 331-340.
[26] M. Nowak, B. Kauch, P. Szperlich, Review of Scientific Instruments, 80 (2009) 046107-046101 - 046107-046103.
[27] E. Manikandan, M.K. Moodley, S. Sinha Rajan, (2010).
[28] J.L. Birman, Theory of Crystal Space Group and Lattice Dynamics, Springer Verlag, Berlin, 1984.
[29] R. Vinodkumar, K.J. Lethy, P.R. Arunkumar, R.R. Krishnan, N.V. Pillai, V.P.M. Pillai, R. Philip, Materials Chemistry and Physics, 121 (2010) 404-413.
[30] M. Ristic, S. Music, M. Ivanda, S. Popovic, Journal of Alloys and Compounds, 397 (2005) L1-L4.
[31] V.V. Ursaki, O. Lupan, I.M. Tiginyanu, G. Chai, L. Chow, Journal of Nanoelectronics and Optoelectronics, 6 (2011) 473-477.
[32] T. Saunder, S. Eisermann, B.K. Meyer, P.J. Klar, Physical Review B, 85 (2012).
[33] D.T. C., S.P.S. Porto, T. Tell, Physical Review 142 (1966) 570-574.
[34] J.M. Calleja, M. Cardona, Physical Review B, 16 (1977) 3753-3761.
[35] J. Zhu, R. Yao, C. Liu, L.-H. Lee, L. Zhu, J.-w. Ju, J.H. Baek, B. Lin, Z. Fu, Thin Solid Films, 514 (2006) 306-309.

[36] S. Ben Yahia, L. Znaidi, A. Kanaev, J.P. Petitet, Spectrochimica Acta Part A: Molecular and Biomolecular Spectroscopy, 71 (2008) 1234-1238.

Table 1

Optical band gap (E_g) of ZnO and 5% Al-ZnO films deposited on glass and n-Si(111) measured by specular and DRS UV-vis results

Substrate	% Al	Annealed Temperature (°)	Specular UV-vis* E_g (eV)	DRS UV-vis# E_g (eV)
Glass	0	-	3.25	-
Glass	0	600	3.25	
Glass	5	-	2.60	3.03
			3.35	
Glass	5	600	3.00	3.19
			3.60	
Si(111)	5	-	-	3.34
Si(111)	5	600	-	3.22

*Tauc and #Kubelka-Munk equations were used to compute results in this table.